Chronobiology International, 2014; 31(9): 1041–1050

ISSN: 0742-0528 print / 1525-6073 online
DOI: 10.3109/07420528.2014.944618

informa
healthcare

ORIGINAL ARTICLE

Dysregulated daily rhythmicity of neuronal resting-state networks in MCI patients

Janusch Blautzik[1], Céline Vetter[2,3], Annalisa Schneider[1], Evgeny Gutyrchik[2,4], Veronika Reinisch[5], Daniel Keeser[1,5], Marco Paolini[1], Ernst Pöppel[2,4,6], Yan Bao[2,4,6], Maximilian Reiser[1], Till Roenneberg[2], and Thomas Meindl[1]

[1]Institute for Clinical Radiology, Ludwig-Maximilian-University, Munich, Germany, [2]Institute of Medical Psychology, Ludwig-Maximilian-University, Munich, Germany, [3]Channing Division of Network Medicine, Brigham and Women's Hospital and Harvard Medical School, Boston, USA, [4]Human Science Centre, Ludwig-Maximilian-University, Munich, Germany, [5]Department of Psychiatry, Ludwig-Maximilian-University, Munich, Germany, and [6]Department of Psychology and Key Laboratory for Machine Perception (MoE), Peking University, Beijing, China

In young healthy participants, the degree of daily rhythmicity largely varies across different neuronal resting-state networks (RSNs), while it is to date unknown whether this temporal pattern of activity is conserved in healthy and pathological aging. Twelve healthy elderly (mean age = 65.1 ± 5.7 years) and 12 patients with amnestic mild cognitive impairment (aMCI; mean age = 69.6 ± 6.2 years) underwent four resting-state functional magnetic resonance imaging scans at fixed 2.5 h intervals throughout a day. Time courses of a RSN were extracted by a connectivity strength and a spatial extent approach performed individually for each participant. Highly rhythmic RSNs included a sensorimotor, a cerebellar and a visual network in healthy elderly; the least rhythmic RSNs in this group included a network associated with executive control and an orbitofrontal network. The degree of daily rhythmicity in aMCI patients was reduced and dysregulated. For healthy elderly, the findings are in accordance with results reported for young healthy participants suggesting a comparable distribution of daily rhythmicity across RSNs during healthy aging. In contrast, the reduction and dysregulation of daily rhythmicity observed in aMCI patients is presumably indicative of underlying neurodegenerative processes in this group.

Keywords: Daily rhythmicity, fMRI, healthy aging, MCI, resting-state networks

INTRODUCTION

In recent years, a growing number of neuroimaging studies focusing on the brain's activity at rest have demonstrated the presence of reproducible resting-state networks (RSNs), which represent brain regions of synchronized low-frequency (0.01–0.1 Hz) fluctuations in the blood oxygen level dependent (BOLD) signal measured by functional magnetic resonance imaging (fMRI) technique (Beckmann et al., 2005; Biswal et al., 2010; Zuo et al., 2010). The spatial patterns of RSNs show, however, strong resemblance with brain networks, which are known from activation studies to be involved in primary and higher order cognitive functions (Laird et al., 2011). The neuronal basis of RSNs has not yet been fully understood; it has been suggested that these functional connectivity patterns may reflect the brain's ongoing intrinsic activity that may be necessary for maintaining its functional integrity (Brookes et al., 2011; He et al., 2008; Pizoli et al., 2011; Shmuel & Leopold, 2008).

Changes within these intrinsic connectivity patterns occur physiologically during life time (Fair et al., 2008; Tomasi & Volkow, 2012) and pathologically in many neuropsychiatric and neurodegenerative disorders (Rocca et al., 2010; Stigler et al., 2011; Verstraete et al., 2010). In particular, the latter fact has drawn much interest into the field of resting-state fMRI due to its potential applicability for clinical purposes. In that context, disruptions of a connectivity pattern referred to as the default-mode network (DMN) (Raichle et al., 2001) have been reported in patients with Alzheimer's disease (AD) (Greicius et al., 2004) as well as in patients with amnestic mild cognitive impairment (aMCI) (Sorg et al., 2007), which is believed to represent a prodromal

Submitted April 16, 2014, Returned for revision July 5, 2014, Accepted July 10, 2014

Correspondence: Dr. Janusch Blautzik, MD, Ziemssenstr. 1, 80639 Munich, Germany. Tel: +49 89 5160 9101. Fax: +49 89 5160 9102. E-mail: janusch.blautzik@med.uni-muenchen.de

stage of AD (Petersen et al., 1999). Moreover, these disruptions have been shown to allow the differentiation between healthy aging, aMCI and AD (Rombouts et al., 2005) as well as between different stages of AD (Zhang et al., 2010), potentially turning the DMN into a novel imaging marker used to detect and follow-up participants at increased risk of developing dementia (Greicius et al., 2004).

More recently, it has been shown that RSNs of young healthy subjects exhibit various levels of systematic daily fluctuations ranging from stable – as in the case of a network associated with the processing of executive control – to highly rhythmic – as in the case of two DMN sub-systems and a sensorimotor network (Blautzik et al., 2013).

In general, systematic fluctuations over the course of the day occur physiologically in virtually all body functions from gene expression (Merrow et al., 2005) to behavior (Roenneberg & Merrow, 2005) and higher cognitive functions (Schmidt et al., 2007). They are caused by an interaction between the circadian timing system or circadian clock and the homeostatic process. The circadian clock actively synchronizes to the Earth's 24-h rotation, mainly by the light/dark cycle, and thereby regulates physiology and behavior (Roenneberg & Merrow, 2005). The phase of synchronization between the external light/dark cycle and an individual's circadian clock is highly individual, giving rise to so-called ''chronotypes'' (Roenneberg et al., 2003). The homeostatic process on the other hand describes the drive for sleep, which steadily accumulates during the wake period (Borbely, 1982).

The current literature demonstrates that daily fluctuations are frequently dysregulated in the central nervous system (and throughout the rest of the body) with healthy aging and – to a greater extent – during age-associated pathologic conditions such as MCI (Naismith et al., 2010) and in particular dementia (Stranahan, 2012). Reasons for this relationship include the deterioration of functional neuronal systems, such as the circadian clock, which occur physiologically with aging and particularly during neurodegenerative processes (Kondratova & Kondratov, 2012). Given this relationship, it may be assumed that aging – both healthy and to a greater extent pathologic – also affects systematic daily fluctuations of RSNs.

From a clinical point of view, i.e. with respect to the potential use of RSNs as tools in the diagnosis or the follow-up of neurodegenerative diseases, knowledge about daily patterns of those systems in normal and pathological aging appears to be necessary for the interpretation of the results derived from resting-state fMRI measurements. For instance, the degree of alterations observed within RSNs during a pathological condition in comparison to a healthy state may vary if differences in daily network dynamics between both conditions exist and the aspect of time of day is disregarded. Moreover, longitudinally assessed changes within RSNs – as for example typically done during follow-up examinations – may derive from physiological daily fluctuations rather than being attributable to pathologic alterations.

To explore this issue, we studied the daily fluctuations of RSNs in healthy elderly representing healthy aging and patients with aMCI as a prodromal stage of dementia representing pathologic aging, while controlling for inter-individual variations in internal time (i.e. chronotype) and time-awake (i.e. the homeostatic process).

MATERIALS AND METHODS

The study was carried out in accordance with the Declaration of Helsinki and was approved by our institutional ethics committee. The experimental protocol was conformed to international ethical standards and methods for the conduct of high-quality animal and human biological rhythm research (Portaluppi et al., 2010). All participants gave their written informed consent and received payment for their participation.

Participants

Twelve healthy elderly volunteers (HC) (five females; mean age = 65.1 ± 5.7 years) and 12 patients with mild cognitive impairment (MCI) (eight females; mean age = 69.6 ± 6.2 years) participated in the study (see Supplemental Information Table 1 for further demographic characteristics). Healthy participants were recruited from an adult education center and had no subjective memory complaints. Amnestic MCI patients were recruited from the university's Memory Clinic and met the Mayo clinic criteria for aMCI (Petersen et al., 2001). They achieved reduced results in the CERAD battery subtests (performed within three months from the fMRI session) consistent with the characterization of this group as aMCI in several cognitive domains: MMSE = 26.25 ± 3.24, verbal fluency = 16.5 ± 5.14, Boston naming test = 14.00 ± 1.53, word list learning = 17.33 ± 5.09, word list recall = 4.75 ± 2.24, word list recognition = 8.25 ± 2.92, constructional praxis = 10.67 ± 2.69 and recall of constructional praxis = 5.00 ± 3.24.

Exclusion criteria for study participation included psychiatric and/or neurological disease, sleep disorders, shift work, psychoactive substance abuse within the last three months, current or previous drug addiction, smoking and intra-corporal ferromagnetic objects. Right-handedness was ensured by a minimum Lateralization Quotient of 70, as assessed with the Edinburgh Inventory (Oldfield, 1971).

Assessment of chronotype

We used the Munich Chronotype Questionnaire to assess chronotype. The questionnaire asks simple questions about an individual's sleep and wake behavior, on both work and free days (if present) (Roenneberg et al., 2007). Chronotype is quantified by an individual's mid-sleep time on free days (MSF) corrected for

potential sleep debt accumulated during the work week; if participants sleep less on work days than on free days, MSF is corrected for ''over-sleep'', resulting in MSF_{sc}:

$$MSF = \text{sleep onset} + (\text{sleep duration on free days})/2$$

$$MSF_{sc} = MSF - \frac{\left\{\begin{array}{l}(\text{sleep duration on free days} \\ \quad - \text{average weekly sleep duration})\end{array}\right\}}{2}$$

(Roenneberg et al., 2003, 2007). Participants' chronotype (MSF_{sc}) ranged from 1:50 to 5:25 a.m.

Study design

Each subject underwent four fMRI scans within a day at fixed 2.5-h intervals. Individual scanning times were adapted to the participant's MSF_{sc} to minimize chronotype differences and to keep time awake between chronotypes as similar as possible. Participants' scanning times were scattered as follows: MSF_{sc} of 1:30–2:30 started at 9 a.m., MSF_{sc} of 2:30–3:30 at 9:30 a.m., MSF_{sc} of 3:30–4:30 at 10 a.m. and finally those with an MSF_{sc} of 4:30–5:30 at 10:30 a.m. This time schedule covered approximately 10 h of the 24 h day. Since the study design did not allow the assessment of similar chronotypes at the same time within a day, measurements were spread out over several weekend days, but scanning times were kept identical for each chronotype category. Given the impact of daylight exposure on the circadian phase and neural activation (Vandewalle et al., 2006), which may have caused unequal inter- and intra-day testing conditions, participants were instructed to stay in the windowless MRI waiting area for the duration of the entire experiment. All scans were performed on five weekends during the winter. In accordance with other resting-state fMRI studies (Beckmann et al., 2005; Damoiseaux et al., 2006; Sorg et al., 2007), participants were instructed to keep their eyes closed without falling asleep and not to think of anything in particular. Snacks and beverages were provided *ad libitum*. Participants were instructed to consume caffeinated beverages just as they used to do on ordinary days.

Functional magnetic resonance imaging

Functional MRI was performed using a 3.0 Tesla Magnetom (VERIO, Siemens, Erlangen, Germany) with a 12-element head coil. For anatomical reference, a sagittal high-resolution magnetization-prepared rapid gradient-echo sequence was acquired with the following imaging parameters: field of view (FoV): 256×256 mm; spatial resolution: $1 \times 1 \times 1$ mm; time of repetition (TR): 2400 ms; time of echo (TE): 3.06 ms; flip angle (FA): 9°; number of slices: 160; acquisition time (TA): 4:45 min. Functional data were recorded using a BOLD sensitive echo-planar gradient-echo sequence in axial orientation (FoV: 192×192 mm; spatial resolution: $3 \times 3 \times 4$ mm; slice gap: 0.4 mm; imaging matrix: 64×64; TR: 3000 ms; TE: 30 ms; FA: 80°; number of slices: 36; TA: 6:06 min). Before starting imaging, 3D-field shimming was performed using automated shimming algorithms implemented on the scanner.

Statistical analyses of fMRI data

The data preprocessing steps were carried out using the software packages FSL (FMRIB Software Library, Oxford, UK), Release 5.0 and Analyses of Functional NeuroImages (AFNI, Bethesda, MD) as described by Biswal et al. (2010): (1) skull removing of individual high-resolution T1-weighted images; (2) motion correction, skull stripping, spatial smoothing applying a 6-mm FWHM Gaussian kernel, band-pass filtering using a high-pass filter of 0.01 Hz and a low-pass filter of 0.1 Hz as well as removing of linear and quadratic trends of 4D functional data sets after discarding the initial five volumes of each 4D functional data set to account for T1 saturation effects; (3) registration and normalization of anatomical and functional data sets to the MNI152 standard space applying a 12 degrees of freedom linear affine transformation (Jenkinson et al., 2002; Jenkinson & Smith, 2001); (4) regression of the functional 4D data sets on global signal, signals derived from cerebrospinal fluid and white matter, and on six motion parameters.

Independent component analysis

Functional MRI data were analyzed with the FSL tools Multivariate Exploratory Linear Optimized Decomposition into Independent Components (MELODIC), version 3.10, and dual-regression (Beckmann et al., 2009; Biswal et al., 2010; Zuo et al., 2010).

In order to generate comparable RSNs in either group and session, the fMRI time-courses derived from all participants (24) and sessions (4) were spatially concatenated in the MNI152 standard space for allowing the estimation of a covariance matrix and the reduction of data *via* Probabilistic Independent Component Analysis as implemented in FSL. Reduced individual data sets were processed with FSL's Temporal Concatenation Group ICA (TC-GICA) to calculate multi-subject multi-session group-level independent components (ICs). In line with previous resting-state fMRI studies (Biswal et al., 2010; Blautzik et al., 2013; Zuo et al., 2010), we used a low order TC-GICA decomposing the data set into 20 group-level ICs.

To be considered RSNs, connectivity patterns were required to extent over functionally relevant brain areas as reported elsewhere (Biswal et al., 2010; Zuo et al., 2010) and to consist predominantly of signals in the frequency range between 0.01 and 0.1 Hz, which have been demonstrated to be characteristic for RSNs using BOLD fMRI (Cordes et al., 2001; Fox et al., 2005; Mantini et al., 2007). Connectivity patterns not meeting these criteria were considered to represent non-neural artificial noise; these artifact patterns were excluded from the subsequent rhythmicity analyses. Dual regression was used to reconstruct the 20 TC-GICA derived group-level ICs into individual ICs for each subject and session.

Assessment of rhythmicity

Analogously to a previously described procedure (Blautzik et al., 2013), we investigated the relative rhythmicity of each connectivity pattern as a function of internal time, i.e. based on hours elapsed since MSF_{sc}. For this purpose, a mean z-value and the number of voxels representing a connectivity pattern's connectivity strength and spatial extent, respectively, were extracted from each individual IC. The connectivity strength approach can be regarded in this case as the mean degree of interaction between voxels within a specific network in an individual without giving information about the spatial properties of that network; on the other hand, the spatial extent approach gives this information without specifying the intra-network connectivity strength. We therefore use connectivity strength and spatial extent as complementary approaches. To ensure the inclusion of statistically relevant voxels into this analysis, i.e. voxels representing a connectivity pattern with a high degree of probability, we defined a threshold of $z \geq 3.0$ for individual ICs, which equals a conservative significance level of $p \leq 0.0027$. Additional analyses for validation purposes were performed using thresholds of $z \geq 2.0$ and $z \geq 4.0$. In order to control for inter-individual differences in baseline connectivity levels, mean z-values and the number of voxels were transformed into % deviations from the respective individual connectivity pattern's average value across all four scan sessions.

The waveform of daily rhythms can in most cases be described by a two-harmonic regression model combining a 24 and a 12 hours component (Brown & Czeisler, 1992). In this study, we modeled the daily time courses of both connectivity strength and spatial extent of each RSN at the group-level for HC and MCI separately by applying the two-harmonic equation

$$f(\psi) = a \cdot \cos(\psi) + b \cdot \sin(\psi) + c \cdot \cos(2\psi) + d \cdot \sin(2\psi) + e$$

(Brown & Czeisler, 1992) to the individual % deviations plotted against h since MSF_{sc}. In this formula, $f(\psi)$ is the periodic signal representing the output of the endogenous circadian pacemaker, a, b, c and d are the coefficients of the cosine and sine harmonics, respectively, and e represents the mean of the % deviation data (Brown & Czeisler, 1992).

This step produced a correlation coefficient r specifying the goodness of fit as well as the range of oscillation, i.e. the maximum of the best fit – the minimum of the best fit, for each RSN in either group. Given that rhythmicity of a signal is characterized by both the goodness of fit and the range of oscillation, both parameters were multiplied by each other to calculate a ''Rhythmicity Index'' (RI); note that RIs were additionally multiplied by 100 for visualization purposes.

In line with a prior work investigating daily rhythmicity in young healthy subjects (Blautzik et al., 2013), the daily time course of a connectivity pattern was considered highly rhythmic if its RI was above 1.5 standard deviations from the average RI across all RSNs. We decided to determine this cut-off upon data derived from healthy elderly only assuming that this group represents healthy aging and therefore exhibits a range of daily RSN rhythmicity that is normal for their age. The corresponding calculation of the lower cut-off, i.e. average RI minus 1.5 standard deviations based on data from healthy elderly, yielded partially negative results; we therefore considered the two lowest ranked RSNs in each group as those with the least rhythmic time courses.

In addition to the rhythmicity analyses, we investigated possible between-group differences in the RI, goodness of fit and range of oscillation values as well as – network specific – in the % deviation data using Student's t-tests. These additional analyses were performed with SPSS Statistics version 22 (IBM, New York, NY).

RESULTS

Healthy elderly and aMCI patients did not significantly differ in age (t-test, $p = 0.09$), gender distribution (Fisher's exact test, $p = 0.41$) and years of education (t-test, $p = 0.33$); there was also no significant between-group difference in the distribution of participants still at work (Fisher's exact test, $p = 0.64$). No significant between-group differences existed in chronotype (results are given as mean ± standard deviation: MSF_{sc} healthy elderly = 3.69 ± 0.64; MSF_{sc} MCI patients = 3.15 ± 0.91; t-test, $p = 0.12$) and the time since MSF_{sc} (time since MSF_{sc} healthy elderly 10.09 ± 2.71; aMCI patients = 10.60 ± 2.84; t-test, $p = 0.38$).

Functional MRI data

The connectivity patterns represented in 15 of the 20 TC-GICA derived group-level ICs were considered RSNs (Figure 1). IC 1 comprised a widespread pattern of connectivity including the prefrontal cortex, the opercular cortex, the putamen and thalamus, the anterior and middle cingulate cortex and the parieto-temporal junction; this pattern resembles a network that has been proposed to play a major role in executive control and working memory function (Beckmann et al., 2005; Laird et al., 2011). Connectivity patterns represented in IC 3, 4 and 11 included sub-systems of the DMN (Laird et al., 2009; Raichle et al., 2001; Zuo et al., 2010); IC 3 showed a posteriorly accentuated sub-network involving the precuneus, the posterior and anterior cingulate cortex, the ventromedial prefrontal cortex, the parietooccipital junction and the thalamus; the sub-network presented in IC 4 was rostrally pronounced and combined the medial prefrontal cortex with the anterior and the posterior cingulate cortex, the precuneus cortex and the caudate; IC 11 encompassed mainly the middle

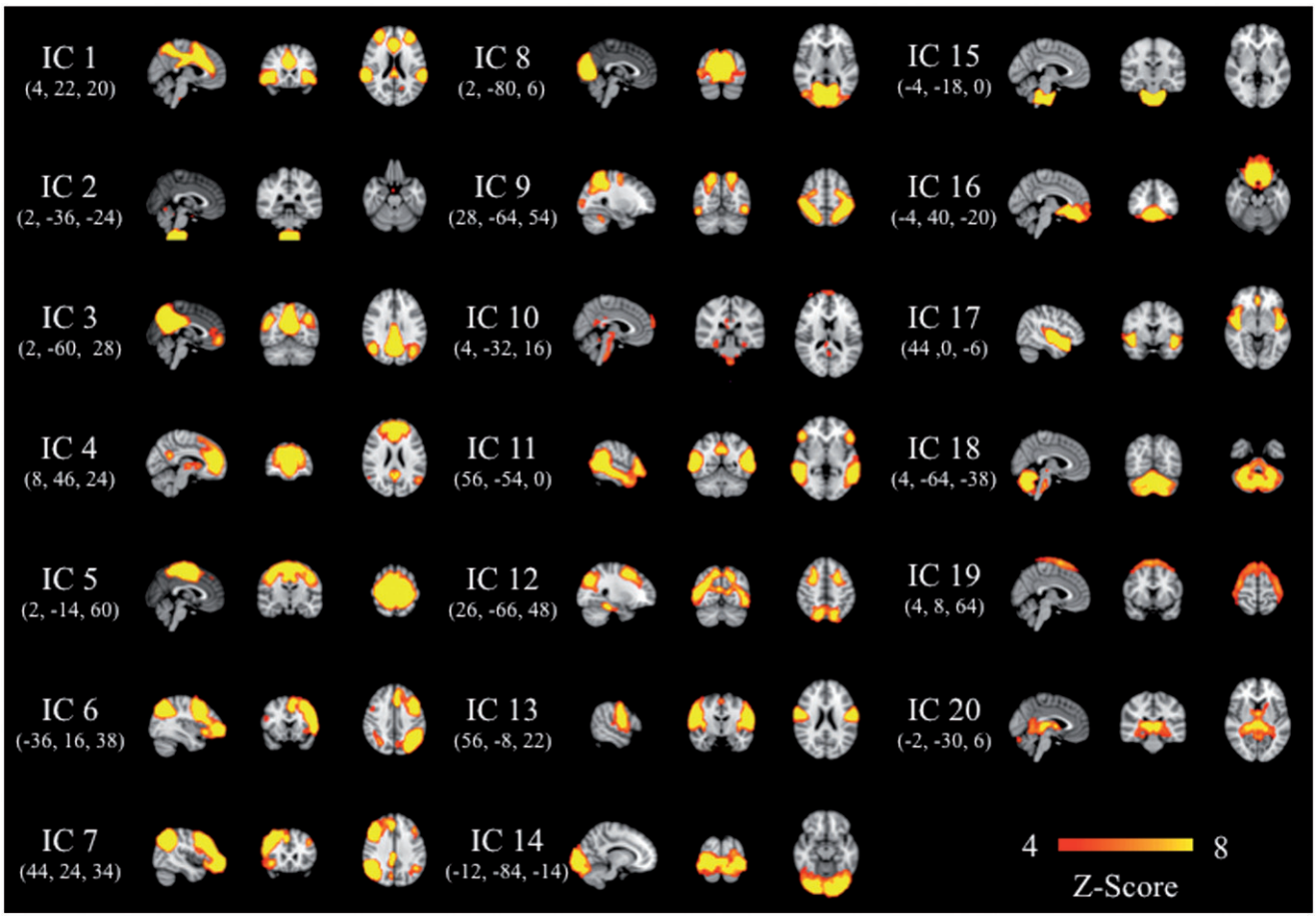

FIGURE 1. Multi-subject multi-session component maps (for all 24 participants and all 4 sessions) as generated by the TC-GICA sorted by the decreasing percentage of variance explained by each component. Sagittal, coronal and axial images are displayed in radiological convention (*x*-, *y*- and *z*-coordinates of each slice in the MNI152 standard space are given in parenthesis). TC-GICA: Temporal Concatenation Group Independent Component Analysis.

temporal gyrus extending into the parieto–temporo–occipital junction, the posterior cingulate and the precuneus cortex as well as the inferior fontal gyrus. IC 5 and 13 involved mainly pre- and postcentral regions and have been described as sensorimotor networks (Biswal et al., 1995, 2010); IC 5 showed a cluster predominantly consisting of the superior parts of the pre- and postcentral gyri and the supplementary motor cortex; IC 11 included the inferior parts of the pre- and postcentral gyri as well as the opercular cortex. IC 6 and 7 both comprised connectivity patterns extending over fronto–temporo–parietal cortex regions (Biswal et al., 2010), which are known to be functionally integrated in a wide range of cognitive processes (Laird et al., 2011); these were the only ICs showing a strong lateralization. Connectivity patterns represented in IC 8 and 14 both extended over the occipital cortex forming visual networks (Biswal et al., 2010); the more medial visual areas were present in IC 8, the more lateral in IC 14. IC 9 demonstrated a pattern extending mainly over the parietal cortex, the lateral occipital cortex, the inferior temporal gyrus and precentral areas; this set of brain regions corresponds to the dorsal attention network (Fox et al., 2006). IC 12 combined frontal regions with the lateral occipital cortex extending into the occipito–temporal junction and the precuneus (Biswal et al., 2010). IC 16 encompassed the orbitofrontal cortex; this pattern resembles a previously described RSN (Biswal et al., 2010; Zuo et al., 2010); however, it may also represent a movement-by-field-inhomogeneity artifact (Andersson et al., 2001; Drobnjak et al., 2006). A pattern extending mainly over the superior temporal lobe representing the auditory cortex was demonstrated in IC 17 (Damoiseaux et al., 2006). A cerebellar pattern with involvement of the thalamus was represented in IC 18 (Biswal et al., 2010; Zuo et al., 2010).

The patterns of the remaining five ICs were assumed to be associated with non-neural noise derived from large vessel (IC 2, 10 and 15) (Dagli et al., 1999; Zuo et al., 2010) or CSF (IC 20) (Lund et al., 2006; Zuo et al., 2010) pulsation and head motion due to cardiac or respiratory pulsation (IC 19) (Dagli et al., 1999; Lund et al., 2006; Zuo et al., 2010).

Rhythmicity analyses

To account for multiple comparisons (15 comparisons for signal strength and spatial extent, respectively, resulting in a total of 30 comparisons), the initial

significance level (α) of 0.05 was Bonferroni corrected resulting in an adjusted α of 0.00167 (Abdi, 2007).

Rhythmicity analyses in healthy elderly

For the connectivity strength approach, the upper RI cut-off resulted in 5.48 (mean RI: 2.57, 1.5 SD: 2.92) (Table 1, left panel). A sensorimotor network (IC 5) and the cerebellar network (IC 18) met the criterion required for high rhythmicity, i.e. an RI above the upper RI cut-off. The connectivity strength of both patterns oscillated in phase showing a convex shape during the day with a peak approximately 12 hours after MSFsc (Supplemental Information Figure 1). A sub-network of the DMN (IC 11) and the network extending over the orbitofrontal cortex (IC 16) were identified as the least rhythmic ones in this group (Table 1, left panel; Supplemental Information Figure 1).

For the spatial extent approach, the upper RI cut-off resulted in 28.93 (mean RI: 15.72, 1.5 SD: 13.21) (Table 1, right panel). The lateral visual network (IC 14) fulfilled the criterion for high rhythmicity; it showed an increase of spatial extent during most of the day peaking approximately 12.5 hours after MSFsc and declining thereafter (Supplemental Information Figure 2). The least rhythmic RSNs included the executive control (IC 1) and the orbitofrontal network (IC 16) (Table 1, right panel; Supplemental Information Figure 2).

Rhythmicity analyses in aMCI patients

None of the RSNs in this group achieved an RI above the upper RI cut-off derived from healthy elderly with regard to both the connectivity strength and the spatial extent approach, i.e. there were no RSNs considered highly rhythmic in this group (Table 2). The least rhythmic networks included a DMN sub-network (IC 3) and the cerebellar network (IC 18) according to the connectivity strength approach, and a sensorimotor (IC 5) and the orbitofrontal network (IC 16) according to the spatial extent approach (Supplemental Information Figure 3).

Also with regard to the supplementary analyses using thresholds of $z \geq 2.0$ and $z \geq 4.0$, no RSN could meet the criterion for high rhythmicity in the group of aMCI patients in either approach (Supplemental Information, Tables 2–5).

Note that there were also no highly rhythmic RSNs in aMCI patients using specific cut-offs based on RIs derived from this group for the connectivity strength and the spatial extent approach (data not shown here).

RI ranking orders

The RI-derived ranking orders in the connectivity strength and spatial extent approaches (using the standard threshold of $z \geq 3.0$) were highly consistent with those calculated for additional thresholds of $z \geq 2.0$ and $z \geq 4.0$ within either group confirming the validity of the results (see Supplemental Information Table 6 for correlation analyses). In case of the healthy elderly group, there was also a significant relationship between the RI ranking orders derived from either approach (Spearman $\rho = 0.67$, $p = 0.006$) demonstrating that distribution of rhythmicity across RSNs was similar across

TABLE 1. Fit parameters, rhythmicity index (RI) and ranking of the connectivity patterns for healthy elderly.

Connectivity strength						Spatial extent					
IC	*r*	*p*	Amp	RI	Rank	IC	*r*	*p*	Amp	RI	Rank
1	0.37	0.0099	0.05	1.84	9	**1**	**0.11**	**0.4639**	**0.11**	**1.18**	**15**
3	0.28	0.0552	0.06	1.63	10	3	0.20	0.1610	0.21	4.21	13
4	0.30	0.0392	0.06	1.94	8	4	0.56	0.0000[a]	0.28	15.62	8
5	0.55	0.0000[a]	0.13	7.36	1	5	0.53	0.0001[a]	0.45	23.84	5
6	0.30	0.0415	0.04	1.27	12	6	0.43	0.0022	0.34	14.92	9
7	0.28	0.0523	0.05	1.28	11	7	0.45	0.0015	0.20	8.77	12
8	0.38	0.0075	0.12	4.63	3	8	0.50	0.0003[a]	0.32	15.81	7
9	0.36	0.0127	0.06	2.09	7	9	0.53	0.0001[a]	0.45	23.93	4
11	**0.21**	**0.1572**	**0.03**	**0.64**	**14**	11	0.28	0.0522	0.31	8.83	11
12	0.36	0.0131	0.08	2.85	5	12	0.56	0.0000[a]	0.47	26.63	3
13	0.46	0.0010[a]	0.06	2.76	6	13	0.50	0.0003[a]	0.28	14.09	10
14	0.31	0.0329	0.09	2.92	4	14	0.48	0.0005[a]	0.60	28.99	1
16	**0.14**	**0.3258**	**0.03**	**0.38**	**15**	**16**	**0.17**	**0.2382**	**0.21**	**3.70**	**14**
17	0.23	0.1228	0.04	0.87	13	17	0.43	0.0025	0.41	17.66	6
18	0.48	0.0005[a]	0.13	6.09	2	18	0.53	0.0001[a]	0.52	27.68	2

Parameters and rankings shown in Tables 1 and 2 are given for the 15 resting-state networks with regard to both connectivity strength (left panel) and spatial extent (right panel). Data are derived from individual ICs thresholded at $z \geq 3.0$. Connectivity patterns meeting the outlier criterion (RI > mean RI + 1.5 standard deviations) are highlighted in gray; those with a significant 2-harmonic fit are marked with an superscript 'a'; note that significance levels were Bonferroni-adjusted for multiple comparisons (total of 30 comparisons in each group, for connectivity strength and spatial extent, resulting in an adjusted alpha level of $p < 0.00167$). The two lowest ranked connectivity patterns according to the RI are marked in bold.

r: coefficient of the fitting function; *p*: significance of the fitting function; Amp: amplitude or range of oscillation of the fitting function (max − min); RI: rhythmicity index ($r \times \text{Amp} \times 100$); rank: rank as a function of RI amongst the 15 networks with 1 indicating the highest level and 15 the lowest level of rhythmicity.

TABLE 2. Fit parameters, rhythmicity index (RI) and ranking of the connectivity patterns for aMCI patients.

Connectivity strength						Spatial extent					
IC	*r*	*p*	Amp	RI	Rank	IC	*r*	*p*	Amp	RI	Rank
1	0.28	0.0535	0.05	1.51	6	1	0.30	0.0384	0.34	10.17	2
3	**0.09**	**0.5351**	**0.01**	**0.12**	**15**	3	0.35	0.0158	0.24	8.24	3
4	0.12	0.4163	0.02	0.29	13	4	0.37	0.0099	0.14	5.37	7
5	0.19	0.2038	0.03	0.55	10	**5**	**0.12**	**0.4258**	**0.08**	**0.92**	**15**
6	0.13	0.3609	0.03	0.40	11	6	0.25	0.0821	0.15	3.84	10
7	0.12	0.4021	0.03	0.35	12	7	0.31	0.0338	0.18	5.65	6
8	0.14	0.3399	0.04	0.58	9	8	0.25	0.0810	0.18	4.69	9
9	0.27	0.0670	0.04	1.09	7	9	0.16	0.2875	0.14	2.24	13
11	0.30	0.0391	0.06	1.88	4	11	0.17	0.2447	0.15	2.63	11
12	0.35	0.0160	0.09	3.23	3	12	0.26	0.0732	0.20	5.10	8
13	0.22	0.1290	0.04	0.97	8	13	0.28	0.0590	0.28	7.77	4
14	0.39	0.0061	0.13	5.00	1	14	0.33	0.0222	0.41	13.68	1
16	0.31	0.0359	0.05	1.52	5	**16**	**0.13**	**0.3727**	**0.11**	**1.42**	**14**
17	0.35	0.0158	0.09	3.29	2	17	0.22	0.1337	0.11	2.39	12
18	**0.11**	**0.4516**	**0.02**	**0.17**	**14**	18	0.26	0.0775	0.23	5.82	5

aMCI: amnestic mild cognitive impairment. Refer footnote of Table 1.

both approaches, i.e. a network with a high degree of rhythmicity according to one approach exhibited also a high degree of rhythmicity according to the other approach; this relationship was not found in the aMCI group (Spearman $\rho = -0.15$, $p = 0.58$) implying a dissociation in the daily fluctuation of connectivity strength and spatial extent.

There were no significant between-group associations in the RI ranking orders for the connectivity strength approach (Spearman $\rho = -0.18$, $p = 0.52$) and the spatial extent approach (Spearman $\rho = -0.068$, $p = 0.81$) indicating a different distribution of rhythmicity across RSNs in either group.

Rhythmicity inter-group comparisons

Based on the connectivity strength approach the correlation coefficients specifying the goodness of fit of the two-harmonic regression model to the % deviation data (r) were significantly higher in the HC group than in the aMCI group (0.33 ± 0.10 vs. 0.22 ± 0.10, $p < 0.01$); the amplitudes derived from the two-harmonic regression model were slightly higher – although not significant – in the HC group (0.07 ± 0.03 vs. 0.05 ± 0.03, $p = 0.11$); this was also the case with the RI values (2.57 ± 1.94 vs. 1.4 ± 1.37, $p = 0.08$).

On the basis of the spatial extent approach, both the correlation coefficients r and the two-harmonic regression model amplitudes were significantly higher in the HC group than those derived from the aMCI group (0.42 ± 0.15 vs. 0.25 ± 0.08, $p < 0.01$; 0.34 ± 0.13 vs. 0.20 ± 0.09, $p < 0.01$); in line with these results, also the RIs were significantly higher in the HC group (15.72 ± 8.80 vs. 5.33 ± 3.37, $p < 0.001$).

The results from this comparison show a reduction of systematic daily fluctuation in the spatial extent of RSNs in aMCI subjects and also a slight trend toward a reduced systematic daily fluctuation in the RSN's connectivity strength in this group.

Between-group differences in the % deviation data of RSNs

Given a total of 30 comparisons (15 comparisons for signal strength and 15 comparisons for spatial extent), the initial significance level (α) of 0.05 was Bonferroni corrected resulting in an adjusted α of 0.00167. At the adjusted α-level there was a statistically significant between-group difference only in case of the % deviation data derived from IC 16 in the spatial extent approach (HC: $27.68 \pm 19.96\%$, aMCI: $13.76 \pm 10.26\%$, $p < 0.0001$) suggesting that the absolute degree of fluctuation is not different between groups for the majority of networks.

DISCUSSION

In this work, we explore systematic daily fluctuations of neuronal RSNs in healthy elderly and patients with aMCI – controlled for internal time and for time awake – based on the assumption that the daily patterns of these systems may be affected by healthy and to a greater extent pathologic aging. Rhythmicity analyses were performed by applying an established two-harmonic regression model to the daily time-courses of each RSN's connectivity strength and spatial extent. Our results demonstrate that RSNs of healthy elderly express different degrees of daily rhythmicity – quantified by a Rhythmicity Index (RI) (Blautzik et al., 2013) – according to both approaches used in this study, i.e. connectivity strength and spatial extent. Networks considered least rhythmic in this group included a sub-system of the DMN (IC 11) based on connectivity strength, a network associated with executive control and working memory function (IC 1) based on spatial extent, and an orbitofrontal network (IC 16) based on both connectivity strength and spatial extent. Highly rhythmic networks included a sensorimotor network (IC 5) and a cerebellar network (IC 18) with regard to connectivity strength as

well as a visual network (IC 14) according to the spatial extent approach. Note that the RI ranking order of RSNs was quiet consistent between both approaches in healthy elderly as demonstrated by a high rank correlation indicating that a stronger systematic fluctuation of a network's connectivity strength time-course was generally accompanied by a stronger systematic fluctuation in the time-course of its spatial extent.

The distribution of the degree of systematic daily fluctuations across RSNs observed in healthy elderly resembles by visual inspection to that recently reported for young healthy subjects (Blautzik et al., 2013) where patterns similar to the sensorimotor network (IC 5) and the cerebellar network (IC 18) from this study also ranged across the most rhythmic RSNs (ICs 11 and 13 in the previous study, ranked 1 and 4 according to connectivity strength, and 3 and 4 according to spatial extent), and a pattern resembling the network associated with executive control and working memory function (IC 1) was least rhythmic (IC 6 in the previous study, ranked 19 and 20, respectively, for a total of 20 ICs). A fundamental difference between both studies, however, is that the posteriorly pronounced DMN subsystem (IC 3) demonstrated to be highly rhythmic in young healthy participants (IC 5 in the previous study, ranked 2 and 1) was not found among the most rhythmic networks in healthy elderly; also, the orbitofrontal network (IC 16) identified to be across the least rhythmic networks in healthy elderly was not that arrhythmic in young healthy participants (IC 20 in the previous study, ranked 9 and 5). On the other hand, the visual network (IC 14) found to be highly rhythmic in healthy elderly only ranged in the mid-level of the RI rank in young subjects (IC 10 in the previous study, ranked 12 and 13).

The observed discrepancy in the degree of systematic daily fluctuation in particular networks between healthy elderly and young healthy subjects may be associated with the physiological degeneration of various brain regions with aging including amongst others control structures of circadian rhythms such as the suprachiasmatic nucleus or the basal forebrain (Hofman & Swaab, 2006; Kondratova & Kondratov, 2012). Age-associated alterations have also been described on the level of RSNs (Lustig et al., 2003). In that context, Tomasi & Volkow (2012) recently reported an association between normal aging and decreases in functional connectivity of networks consisting of long-range connections as the DMN and the orbitofrontal cortex, as well as increases in functional connectivity of networks consisting of short-range connections as somatosensory and cerebellar networks. Assuming that strong connectivity within a network of brain regions facilitates their interaction and therefore possibly the synchronization of rhythmic behavior within that network, one would expect that a decrease in the connectivity of an RSN is accompanied by a decrease in its rhythmic behavior. Given this thought, we hypothesize that the observed reduction of systematic daily fluctuation in the posteriorly pronounced DMN sub-system as well as in the orbitofrontal network of healthy elderly may be caused – in addition to alterations within circadian rhythm modulating structures – by an age-related decrease in functional connectivity within these networks; on the other hand, the highly rhythmic behavior within the sensorimotor, visual and cerebellar networks may be related to preserved or increased functional connectivity within these areas with normal aging.

Unlike the findings in healthy elderly, there were no highly rhythmic RSNs according to our criteria in aMCI patients. The least rhythmic RSNs in this group included the posteriorly pronounced sub-system of the DMN (IC 3) and the cerebellar network (IC 18) with regard to connectivity strength as well as the sensorimotor network (IC 5) and the orbitofrontal network (IC 16) with regard to spatial extent. No association between the RI ranking orders derived from both approaches could be observed in aMCI patients indicating that the degree of network rhythmicity dissociates between connectivity strength and spatial extent in this group. Moreover, the RI ranking order was significantly different in aMCI patients from that in healthy elderly for each approach suggesting that the degree of network rhythmicity in this group additionally dissociates from that in healthy elderly. Furthermore, we observed significantly lower RI values in aMCI patients, i.e. lower rhythmicity of RSNs according to the spatial extent approach and a trend toward lower RI values according to the connectivity strength approach. Regarding spatial extent, the lower RI values were based on both significantly lower *r*-values specifying the goodness of fit of the two-harmonic regression model and significantly lower amplitudes of the two-harmonic regression model. Significantly lower goodness of fit of the regression model was also observed in aMCI patients with respect to connectivity strength; note in that context that restricting the *z*-values by using a cut-off and therefore decreasing the variability of data may have contributed to the non-significant between-group differences in RI and amplitude using the connectivity strength approach.

It has to be noted that unlike the rhythmicity intergroup comparison based on the two-harmonic regression model, the underlying % deviation data were not different between groups except of the orbitofrontal network (IC 16) in case of the spatial extent approach that showed significantly lower values in aMCI subjects. These differing findings demonstrate that the absolute degree of fluctuation in a majority of RSNs is not different in aMCI subjects but furthermore becomes unsystematic or dysregulated. Note in that context that the significant difference in % data derived from IC 16 may be linked to a potential artificial origin of that network (Andersson et al., 2001; Drobnjak et al., 2006).

Assuming that the results achieved for healthy elderly represent an age-related physiological condition, we speculate that the observed dysregulation of systematic daily RSN fluctuation in the aMCI group may mirror a

pathologic progression of neurodegenerative processes including the deterioration of functional systems in these subjects. In line with this assumption, several studies have reported progressive disruptions of functional connectivity in aMCI subjects, especially with regard to the DMN (Greicius et al., 2004; Rombouts et al., 2005; Sorg et al., 2007; Zhang et al., 2010). A progressive disruption of the functional architecture, however, would possibly impede the interaction within RSNs resulting in a dysregulation of systematic daily fluctuations of these systems as observed in this study. Given the translational state of MCI between healthy aging and dementia such as AD (Petersen et al., 1999), we speculate that the demonstrated findings may be of an even more severe dimension with progression of the disease, i.e. conversion to dementia.

However, it's noteworthy that dependencies between healthy and pathologic aging, age-associated cognitive decline and dysfunctions of the circadian system are not fully understood since dysfunctions of the circadian system may also contribute to and even precede the development of MCI and dementia (Kondratova & Kondratov, 2012; Tranah et al., 2011). Further studies are therefore needed in order to develop a comprehensive understanding of the processes leading to circadian dysfunction and cognitive decline/dementia in older people and their interactions.

With regard to the results derived from resting-state fMRI studies, our findings indicate that in case of healthy elderly and MCI subjects time of day should not be that important for scanning when concentrating on less rhythmic networks as the DMN. On the other hand, systematic daily fluctuations in highly rhythmic networks as the sensorimotor, cerebellar and visual network may have an impact on the results of longitudinal fMRI studies performed on healthy elderly when ignoring time of day and the participants' chronotype; moreover, potential differences within these networks between healthy elderly and MCI subjects could be influenced or caused by the time of day of the measurement.

A potential limitation of this work may include the absence of controlling the wakefulness of participants during the fMRI resting-state scan as recent research demonstrated that wakefulness of subjects may significantly fluctuate during a resting-state scan and – if not monitored and modeled – have an impact on the functional connectivity architecture (Tagliazucchi & Laufs, 2014). It is therefore possible that out findings may have been influenced by these fluctuations.

We conclude that RSNs of healthy elderly exhibit various levels of systematic daily fluctuations comparable to that found in young healthy participants suggesting a comparable distribution of the degree of daily rhythmicity across RSNs during healthy aging. An exception to this are specific networks as the DMN, which exhibit a less rhythmic behavior during normal aging, potentially caused by age-associated decreases of the long-range connections within these systems. In comparison, systematic daily fluctuations of RSNs are dysregulated in MCI patients, presumably due to progressive neurodegenerative processes including the disruption of resting-state functional connectivity. Dysregulation of daily rhythmicity of RSNs in these patients may reflect at the neuronal level the disturbances of the circadian system frequently observed in subjects with age-associated cognitive decline and neurodegenerative disorders including AD.

ACKNOWLEDGMENTS

The authors thank Isabella Peres and Petra Carl for excellent organizational assistance and Dirk Spannhake for his competent work.

DECLARATION OF INTEREST

The authors report no conflicts of interest.

A grant from the university's own FoeFoLe program funded this research (Grant number 651).

REFERENCES

Abdi H. (2007). Bonferroni and Sidak corrections for multiple comparisons. In: Salkind NJ, ed. Encyclopedia of measurement and statistics. Thousand Oaks, CA: Sage, pp. 105–6.

Andersson JL, Hutton C, Ashburner J, et al. (2001). Modeling geometric deformations in EPI time series. Neuroimage. 13:903–19.

Beckmann CF, DeLuca M, Devlin JT, Smith SM. (2005). Investigations into resting-state connectivity using independent component analysis. Philos Trans R Soc Lond B Biol Sci. 360: 1001–13.

Beckmann CF, Mackay CE, Filippini N, Smith SM. (2009). Group comparison of resting-state FMRI data using multi-subject ICA and dual regression. OHBM poster.

Biswal B, Yetkin FZ, Haughton VM, Hyde JS. (1995). Functional connectivity in the motor cortex of resting human brain using echo-planar MRI. Magn Reson Med. 34:537–41.

Biswal BB, Mennes M, Zuo XN, et al. (2010). Toward discovery science of human brain function. Proc Natl Acad Sci USA. 107: 4734–9.

Blautzik J, Vetter C, Peres I, et al. (2013). Classifying fMRI-derived resting-state connectivity patterns according to their daily rhythmicity. Neuroimage. 71:298–306.

Borbely AA. (1982). A two process model of sleep regulation. Hum Neurobiol. 1:195–204.

Brookes MJ, Woolrich M, Luckhoo H, et al. (2011). Investigating the electrophysiological basis of resting state networks using magnetoencephalography. Proc Natl Acad Sci USA. 108:16783–8.

Brown EN, Czeisler CA. (1992). The statistical analysis of circadian phase and amplitude in constant-routine core-temperature data. J Biol Rhythms. 7:177–202.

Cordes D, Haughton VM, Arfanakis K, et al. (2001). Frequencies contributing to functional connectivity in the cerebral cortex in ''resting-state'' data. AJNR Am J Neuroradiol. 22:1326–33.

Dagli MS, Ingeholm JE, Haxby JV. (1999). Localization of cardiac-induced signal change in fMRI. Neuroimage. 9:407–15.

Damoiseaux JS, Rombouts SA, Barkhof F, et al. (2006). Consistent resting-state networks across healthy subjects. Proc Natl Acad Sci USA. 103:13848–53.

Drobnjak I, Gavaghan D, Suli E, et al. (2006). Development of a functional magnetic resonance imaging simulator for modeling realistic rigid-body motion artifacts. Magn Reson Med. 56: 364–80.

Fair DA, Cohen AL, Dosenbach NU, et al. (2008). The maturing architecture of the brain's default network. Proc Natl Acad Sci USA. 105:4028–32.
Fox MD, Corbetta M, Snyder AZ, et al. (2006). Spontaneous neuronal activity distinguishes human dorsal and ventral attention systems. Proc Natl Acad Sci USA. 103:10046–51.
Fox MD, Snyder AZ, Vincent JL, et al. (2005). The human brain is intrinsically organized into dynamic, anticorrelated functional networks. Proc Natl Acad Sci USA. 102:9673–8.
Greicius MD, Srivastava G, Reiss AL, Menon V. (2004). Default-mode network activity distinguishes Alzheimer's disease from healthy aging: Evidence from functional MRI. Proc Natl Acad Sci USA. 101:4637–42.
He BJ, Snyder AZ, Zempel JM, et al. (2008). Electrophysiological correlates of the brain's intrinsic large-scale functional architecture. Proc Natl Acad Sci USA. 105:16039–44.
Hofman MA, Swaab DF. (2006). Living by the clock: The circadian pacemaker in older people. Ageing Res Rev. 5:33–51.
Jenkinson M, Bannister P, Brady M, Smith S. (2002). Improved optimization for the robust and accurate linear registration and motion correction of brain images. Neuroimage. 17:825–41.
Jenkinson M, Smith S. (2001). A global optimisation method for robust affine registration of brain images. Med Image Anal. 5:143–56.
Kondratova AA, Kondratov RV. (2012). The circadian clock and pathology of the ageing brain. Nat Rev Neurosci. 13:325–35.
Laird AR, Eickhoff SB, Li K, et al. (2009). Investigating the functional heterogeneity of the default mode network using coordinate-based meta-analytic modeling. J Neurosci. 29: 14496–505.
Laird AR, Fox PM, Eickhoff SB, et al. (2011). Behavioral interpretations of intrinsic connectivity networks. J Cogn Neurosci. 23: 4022–37.
Lund TE, Madsen KH, Sidaros K, et al. (2006). Non-white noise in fMRI: Does modelling have an impact? Neuroimage. 29:54–66.
Lustig C, Snyder AZ, Bhakta M, et al. (2003). Functional deactivations: Change with age and dementia of the Alzheimer type. Proc Natl Acad Sci USA. 100:14504–9.
Mantini D, Perrucci MG, Del Gratta C, et al. (2007). Electrophysiological signatures of resting state networks in the human brain. Proc Natl Acad Sci USA. 104:13170–5.
Merrow M, Spoelstra K, Roenneberg T. (2005). The circadian cycle: Daily rhythms from behaviour to genes. EMBO Rep. 6:930–5.
Naismith SL, Rogers NL, Hickie IB, et al. (2010). Sleep well, think well: Sleep-wake disturbance in mild cognitive impairment. J Geriatr Psychiatry Neurol. 23:123–30.
Oldfield RC. (1971). The assessment and analysis of handedness: The Edinburgh inventory. Neuropsychologia 9:97–113.
Petersen RC, Doody R, Kurz A, et al. (2001). Current concepts in mild cognitive impairment. Arch Neurol. 58:1985–92.
Petersen RC, Smith GE, Waring SC, et al. (1999). Mild cognitive impairment: Clinical characterization and outcome. Arch Neurol. 56:303–8.
Pizoli CE, Shah MN, Snyder AZ, et al. (2011). Resting-state activity in development and maintenance of normal brain function. Proc Natl Acad Sci USA. 108:11638–43.
Portaluppi F, Smolensky MH, Touitou Y. (2010). Ethics and methods for biological rhythm research on animals and human beings. Chronobiol Int. 27:1911–29.
Raichle ME, MacLeod AM, Snyder AZ, et al. (2001). A default mode of brain function. Proc Natl Acad Sci USA. 98:676–82.
Rocca MA, Valsasina P, Absinta M, et al. (2010). Default-mode network dysfunction and cognitive impairment in progressive MS. Neurology. 74:1252–9.
Roenneberg T, Kuehnle T, Juda M, et al. (2007). Epidemiology of the human circadian clock. Sleep Med Rev. 11:429–38.
Roenneberg T, Merrow M. (2005). Circadian clocks – The fall and rise of physiology. Nat Rev Mol Cell Biol. 6:965–71.
Roenneberg T, Wirz-Justice A, Merrow M. (2003). Life between clocks: Daily temporal patterns of human chronotypes. J Biol Rhythms. 18:80–90.
Rombouts SA, Barkhof F, Goekoop R, et al. (2005). Altered resting state networks in mild cognitive impairment and mild Alzheimer's disease: An fMRI study. Hum Brain Mapp. 26: 231–9.
Schmidt C, Collette F, Cajochen C, Peigneux P. (2007). A time to think: Circadian rhythms in human cognition. Cogn Neuropsychol. 24:755–89.
Shmuel A, Leopold DA. (2008). Neuronal correlates of spontaneous fluctuations in fMRI signals in monkey visual cortex: Implications for functional connectivity at rest. Hum Brain Mapp. 29:751–61.
Sorg C, Riedl V, Muhlau M, et al. (2007). Selective changes of resting-state networks in individuals at risk for Alzheimer's disease. Proc Natl Acad Sci USA. 104:18760–5.
Stigler KA, McDonald BC, Anand A, et al. (2011). Structural and functional magnetic resonance imaging of autism spectrum disorders. Brain Res. 1380:146–61.
Stranahan AM. (2012). Chronobiological approaches to Alzheimer's disease. Curr Alzheimer Res. 9:93–8.
Tagliazucchi E, Laufs H. (2014). Decoding wakefulness levels from typical fMRI resting-state data reveals reliable drifts between wakefulness and sleep. Neuron. 82:695–708.
Tomasi D, Volkow ND. (2012). Aging and functional brain networks. Mol Psychiatry. 17:549–58.
Tranah GJ, Blackwell T, Stone KL, et al.; Group, S.O.F.R. (2011). Circadian activity rhythms and risk of incident dementia and mild cognitive impairment in older women. Ann Neurol. 70: 722–32.
Vandewalle G, Balteau E, Phillips C, et al. (2006). Daytime light exposure dynamically enhances brain responses. Curr Biol. 16: 1616–21.
Verstraete E, van den Heuvel MP, Veldink JH, et al. (2010). Motor network degeneration in amyotrophic lateral sclerosis: A structural and functional connectivity study. PLoS One. 5:e13664.
Zhang HY, Wang SJ, Liu B, et al. (2010). Resting brain connectivity: Changes during the progress of Alzheimer disease. Radiology. 256:598–606.
Zuo XN, Kelly C, Adelstein JS, et al. (2010). Reliable intrinsic connectivity networks: Test-retest evaluation using ICA and dual regression approach. Neuroimage. 49:2163–77.

Supplementary material available online

Supplementary Figures 1–3; Tables 1–6

Notice of Correction:
Changes to the affiliations of authors eight and nine have been made following the original online publication date of August 6, 2014.